Experimental investigation of in-plane loaded timber-framed rammed earth panels. Part II: cyclic shear-compression tests

Vasilii Baleca[1], Riccardo Barsotti[2], Stefano Bennati[1], Daniel V. Oliveira[3]

[1] Department of Civil and Industrial Engineering, University of Pisa, 56122 Pisa, Italy
[2] Corresponding author, email riccardo.barsotti@unipi.it, Department of Civil and Industrial Engineering, University of Pisa, 56122 Pisa, Italy
[3] Department of Civil Engineering, ISISE, University of Minho, 4800-058 Guimarães, Portugal

Abstract
Preliminary indications about the timber-framed rammed earth panel (TREP) stiffness and load bearing capacity have been obtained from a first experimental study that has been expressively set up and performed to investigate the TREP in-plane static behavior. The present part II, together with the foregoing part I (companion paper), illustrates and discusses the key experimental results obtained from the compression-shear loading tests performed on rammed earth panels reinforced by a contouring timber frame. In the present part II of the paper, the cyclic loading tests on two TREP elements and one bare timber frame are carefully analyzed, the results are discussed, in terms of load capacity and ductility, and the detected damage modes are explained. The results seem to show that the reinforcing timber frame provides a substantial benefit enabling the development of an effective "strut-and-tie" resisting mechanism that effectively exploits the compressive strength of the rammed earth panel and promotes a ductile failure mode.

1. Introduction
The use of earth as a building material is certainly one of the oldest techniques practiced in the history of humanity. The architecture of ancient Egypt, the Middle East, China, Central Asia, Latin America but also Central Europe have been characterized, since ancient times, by this material. As an example, evidence of earthen construction dating back to around 6000 years BC has been found in Anatolia, Turkey, Palestine, and Israel [1].
Over the centuries, the practical experience in the use of this material, handed down from generation to generation, has led to the development of construction rules and ways of building that have declined in different forms in different geographical regions, adapting to different environmental and climatic conditions. Nevertheless, the traditional construction techniques using earth, beyond the specificities linked to the geographical location, possess a series of common distinctive characteristics which, in modern terms, can be summarized under the term "sustainable building".
Nowadays, the reduction of the energy consumption of in all the phases of the building process, from the beginning to the end of life, and more generally of its impact on natural resources and on the environment, are becoming increasingly important, given the increasing attention paid to the issue of sustainable development, also very relevant in the construction sector. Building materials are required to be healthy, non-toxic, recyclable, presenting low embodied energy and able to promote a comfortable climate inside homes. Earth as a building material naturally possesses these qualities and this has fueled a renewed interest of a part of contemporary architecture in this material which, after being set aside in favor of more modern materials, is now being reconsidered in a new light [2].
Earth walls of sufficient thickness can safely withstand vertical loads as long as the height of the building is not excessive. However, when the wall is called upon to resist horizontal actions of a certain entity, the response may not be satisfactory, as happens, more generally, for buildings made with poor quality masonry. In this regard, the traditional

construction techniques that have been developed over time in the different areas of the planet most exposed to seismic actions have produced solutions characterized by the combined use of masonry and wooden reinforcement elements [3] [4].
Taking inspiration from the solutions expressed by traditional construction techniques, this paper illustrates a first experimental investigation of the mechanical behavior of a structural element formed by a rammed earth panel reinforced with wooden elements, called "TREP" (Timber-Frame-Rammed-Earth Panel). The experimental campaign focused on the response of TREP elements to loads acting in their middle plane.
The present contribution is the second part of a two-parts paper illustrating experimental results obtained from the monotonic and cyclic compression-shear loading tests performed on rammed earth panels reinforced by a contouring timber frame. The present part II of the paper deals mainly with the cyclic loading tests and it is organized as follows. Section 2 describes the Timber-Framed Rammed Earth Panel (TREP) that has been designed and built specifically for the test. Section 3 illustrates the experimental campaign and describes in detail the two compression-shear cycling loading tests on the TREP elements, as well as the shear tests on the bare timber frames (TF). The main results obtained from the tests are shown and discussed in Section 4, while a detailed survey of the damage in the panel and in the timber frame is provided in Section 5.

2. Timber-Framed Rammed Earth Panel (TREP)

The main characteristics and construction phases of the TREP elements made of rammed earth panels and reinforced with wooden elements have been carefully described in the part I of the paper [5] and are briefly recalled for the sake of clarity.
The soil used as earth material was obtained in the Alentejo region, located in the south of Portugal. The soil was mixed with gravel and sand to bring the mixture as close as possible to the grain size curve recommended in the literature.

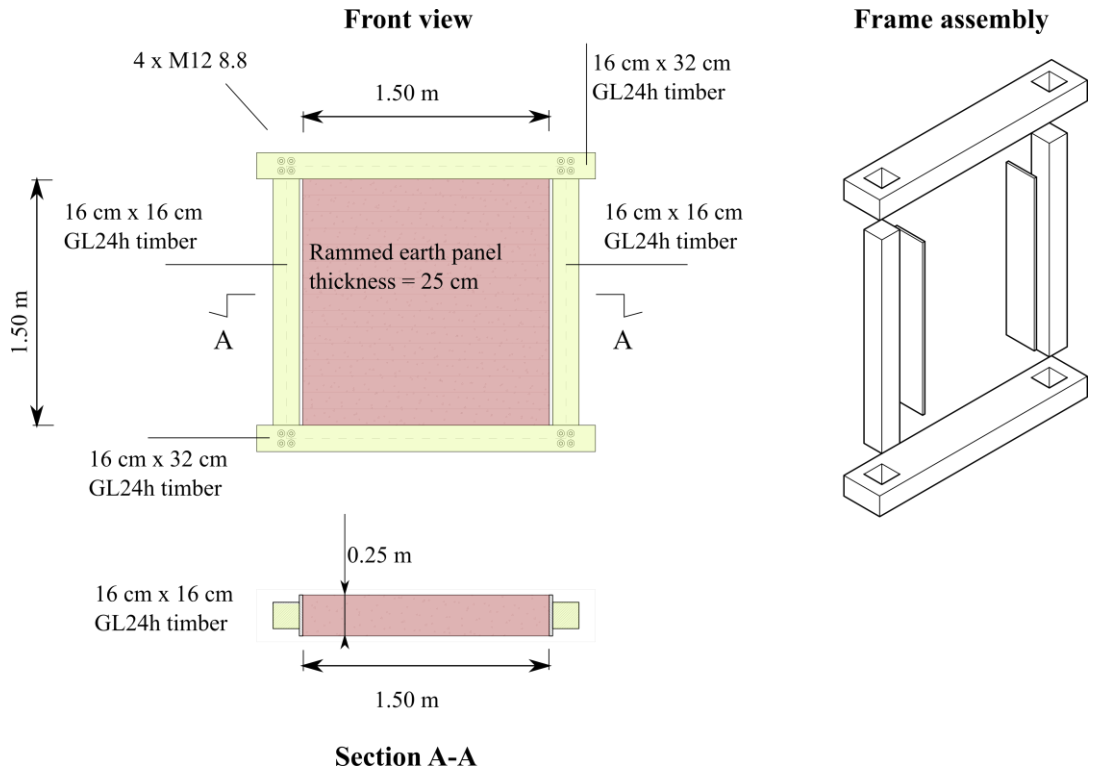

Figure 1: shape and dimensions of the TREP element.

The rammed earth panel has the dimensions of 150 x 150 x 25 cm^3 and is surrounded by a frame made up of prismatic timber elements: two beams with a cross-section of 32 x 16 cm^2 and two columns with a cross-section of 16 x 16 cm^2. Two additional boards of 2 cm width were added along the two side columns to properly confine the earth. The beams and columns of the timber frame are connected by four M12 class 8.8 bolts at each corner (Figure 1).

Assemblage of the TREP elements and execution of the experimental tests were carried out at the Department of Civil Engineering of the University of Minho, Guimarães, Portugal.
The construction of the TREP element begins with the assembly of the lower beam and the two side columns of the wooden frame. The two side columns are inserted into the specifically prepared cavities in the lower beam and are then connected by bolts (Figure 2a). Subsequently, the wooden formwork is installed, and the earth panel is built according to the rammed earth technique (pisé) [6], [7]. The earth material is placed in layers, each having an initial thickness of 15 cm and rammed manually using a wooden mallet (Figure 2b). When the earth panel is complete, the upper timber beam is installed and left un-bolted until the vertical compression is applied to the TREP element (Figure 2c). For a more detailed description of the TREP element assemblage, the reader is referred to [5].

a) *b)* *c)*

Figure 2: construction phases of the TREP element in chronological order from (a) to (c).

The experimental campaign involved the construction of four TREP panels and three bare timber frames, named TF. The three TF are readily built by the simultaneous assembly of beams and columns. The timber elements are connected by the same bolted joints (Figure 3) as in the TREP elements.

a) b) c)

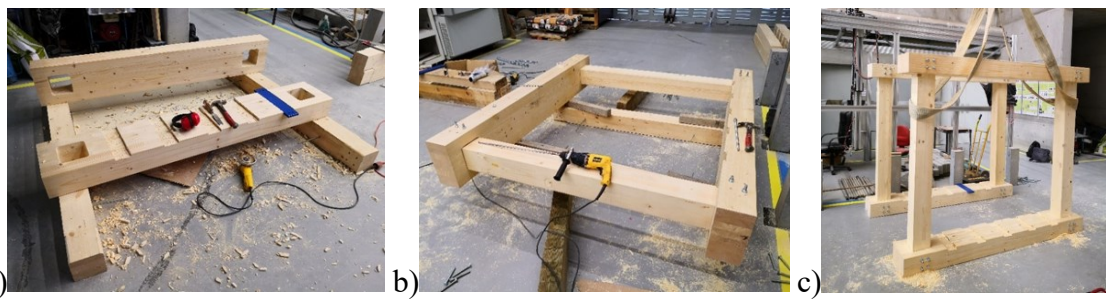

Figure 3: construction phases of the TF element in chronological order from (a) to (c).

3. Experimental campaign

The experimental campaign focused on the TREP in-plane behavior under shear-compression load conditions. A total of four rammed earth panels reinforced with timber elements (TREP1, TREP2, TREP3 and TREP4), and three timber frames without earth filling (TF1, TF2 and TF3) were built for the tests. The test program included:

- two monotonic shear load tests carried out on the bare wooden frames TF1 and TF2; the horizontal load was imposed under monotonic displacement control.
- two monotonic shear-compression load tests carried out on TREP1 and TREP2 elements; the vertical load was kept constant whereas the horizontal load was imposed under displacement control.
- one cyclic shear load test carried out on the TF3 wooden frame; the horizontal load was imposed under displacement control.
- two cyclic shear-compression load tests on TREP3 and TREP4 elements; the vertical load was kept constant while the horizontal load was imposed under cyclic displacement control.

The results obtained from the monotonic tests were used to define the loading protocols for the subsequent cyclic tests. The monotonic loading tests have been discussed in detail in the previous part I [5]; the cyclic tests form the object of the present part II of the paper.

3.1 Experimental setup of the TREP cyclic shear-compression tests

The arrangement of the transducers on the TREP3 and TREP4 specimens and the set-up for the cyclic tests, illustrated in Figure 4, are similar to those adopted for the monotonic tests. However, analysis of the results of the previous monotonic tests enabled optimizing the total number of transducers, reducing it from 39 to 33. The sampling rate for the LVDT has been set to 4 Hz.

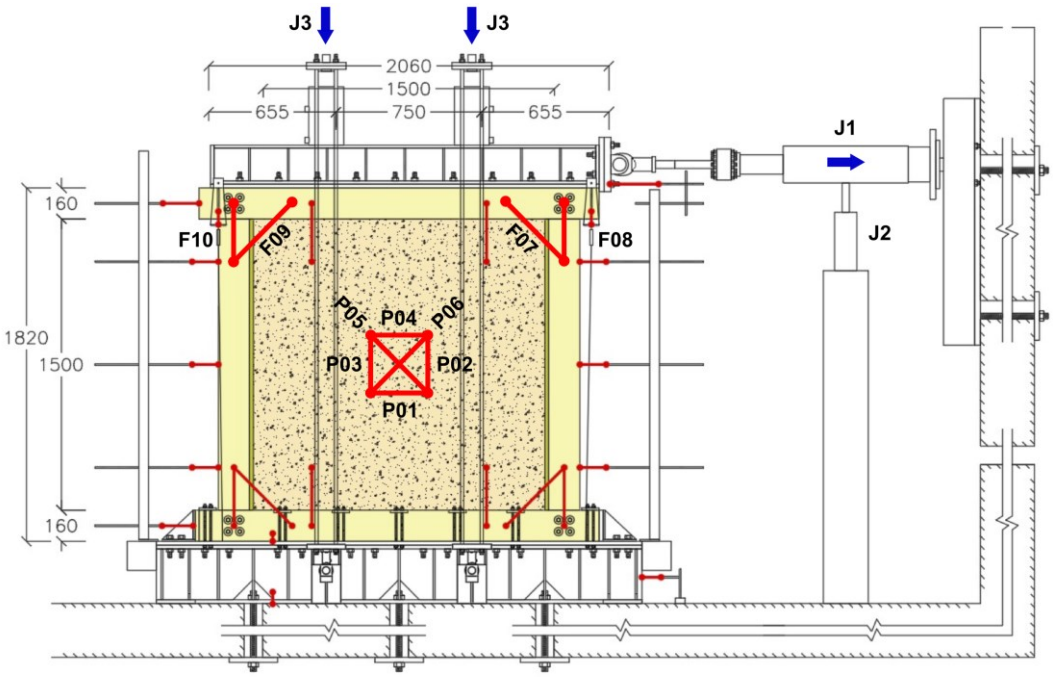

Figure 4: set-up of the tests on TREP3 and TREP4 specimens (dimensions in mm).

The horizontal load is imposed by the "J1" jack having a capacity of 300 kN and a range of ± 200 mm. The test is carried out by progressively increasing the displacement of the jack head "J1" at a constant speed of 0.05 mm/s. A compressed air piston "J2" is placed below jack "J1" to keep it horizontal. A constant vertical load of 50 kN is applied to the upper steel beam by means of two manually controlled jacks labelled "J3". It must be specified that before starting the cyclic test, a vertical preload force was applied to the TREP element by the vertical jacks "J3". The vertical preload force equal to 50 kN was used to ensure the contact condition between the timber frame and the earth panel. It should be noted that the upper timber beam was connected to the columns by inserting and tightening the bolts only after the desired vertical preload was applied.
The TREP specimens are innovative structural systems for which no specific standard is available concerning the definition of the cyclic test load protocol. Consequently, an *ad-hoc* load protocol has been designed by making use of the results obtained from the monotonic tests on the TREP1 and TREP2 elements, as well as by referring to the load protocols established in international standards for cyclic tests, somewhat related to [8], [9]. Due to technical and logistical laboratory restrictions, each load step was composed of one cycle and no inversion of the horizontal load has been performed during the test. The set of cyclic tests described in the following should be intended as a first experimental investigation of the in-plane cyclic behavior of TREP elements. The results obtained from this first analysis will allow for refining and tailoring the design of the load protocol in the following steps of the research. However, the results obtained enable characterizing the main characteristic features of the cyclic behavior of TREP elements.
In the setting up of the load protocol it was assumed that the force-displacement curves of the cyclic tests on the TREP3 and TREP4 elements can be inferred from the monotonic tests on the TREP1 and TREP2 elements; moreover, a progressive stiffness decrease of TREP3 and TREP4 specimens at each cycle has been assumed. Furthermore, only one cycle for each loading-unloading phase has been planned up to a maximum of 10 cycles. The horizontal load is applied by pulling the TREP specimens. A quasi-static movement of the jack during the loading phase (0.05 mm/s) is chosen so as not to damage the panel excessively, while the speed is doubled during the unloading phase to speed up the test. The load protocol adopted for the cyclic tests on the TREP3 and TREP4 elements is shown in Table 1.

Step	Expected target displacements in loading (mm)	Target force at unloading (kN)	Number of cycles	Displ. rate in loading (mm/s)	Displ. rate in unloading (mm/s)
1	4.0	5.0	1	0.05	0.05
2	8.0	5.0	1	0.05	0.05
3	15.0	5.0	1	0.05	0.05
4	30.0	5.0	1	0.05	0.10
5	45.0	5.0	1	0.05	0.10
6	60.0	5.0	1	0.05	0.10
7	75.0	5.0	1	0.05	0.10
8	90.0	5.0	1	0.05	0.10
9	105.0	5.0	1	0.05	0.10
10	120.0	5.0	1	0.05	0.10

Table 1: load protocol for the cyclic tests of the TREP3 and TREP4 elements.

3.2 Experimental setup of the TF shear tests

The TREP mechanical behavior is the result of the complex interaction between the rammed earth panel and the reinforcing timber frame. Hence, investigation of the bare frame response to the applied load is relevant as it enables highlighting the contribution of the reinforcing frame to the system's stiffness and load capacity. In this regard, the experimental campaign comprised two monotonic tests (TF1 and TF2) and one cyclic test (TF3) on the timber frames. The monotonic tests have been illustrated in the part I of the paper [5]; in the following, the cyclic test on the TF3 frame will be described. Before the tests, a total of 23 transducers were installed on the TF frames. The test setup and the positioning of the LVDTs on the TF frames are shown in Figure 5. These tests were performed under displacement control.

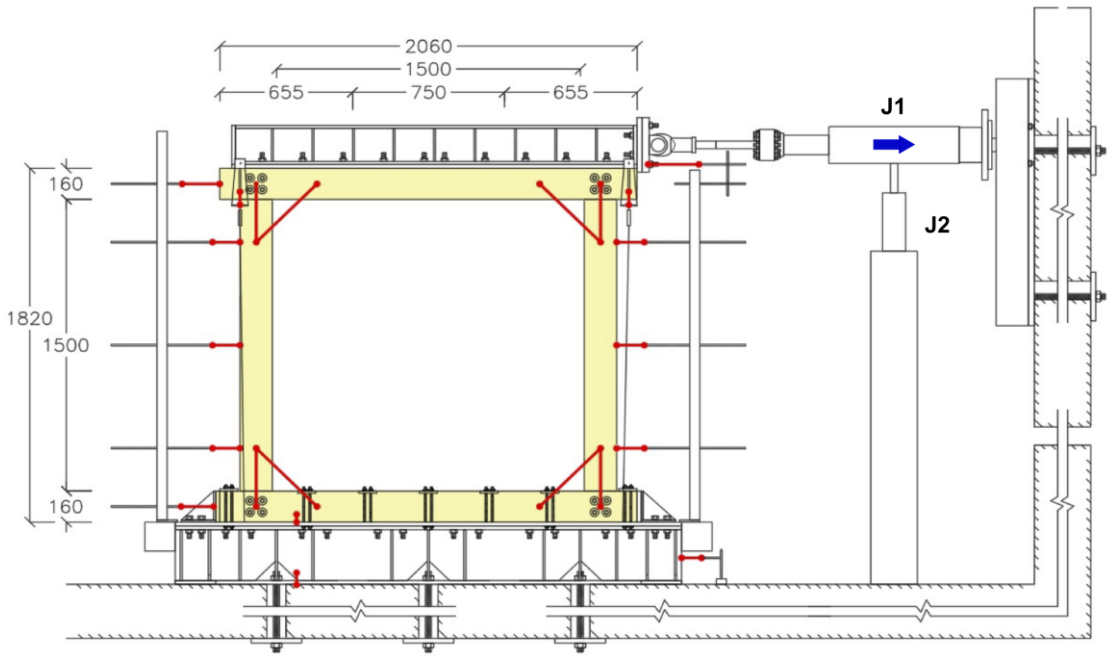

Figure 5: test set-up of the TF3 timber frame.

The horizontal load was imposed using the compressed air jack "J1" having a capacity of 300 kN and a range of ± 200 mm. The tests on the two timber frames were carried out by controlling the jack head displacement. A compressed air piston "J2" has been placed beneath the horizontal jack "J1" to support its weight. The horizontal jack exerted a traction-release force during the cyclic test on the TF3 bare frame, to avoid undesirable out-of-plane displacements.

Thanks to the results obtained from the two monotonic shear load tests in terms of load-displacement curves, and by adopting hypotheses analogous to those already stated for the load protocol of the TREP3 and TREP4 elements, it was possible to calibrate the load protocol for the TF3 bare frame. This time around, the TF frames were expected to have bigger displacements than TREP elements and a remarkably lower stiffness. Compared to the cyclic loading protocol for the TREP elements, it was decided to reduce the number of load cycles and to increase the displacement imposed by the horizontal jack "J1". It was also decided to increase the loading and unloading speed of the jack as brittle failure of the frame could be excluded. Table 2 shows the cycling load protocol for the TF3 frame.

Step	Expected target displacements in loading (mm)	Target force in unloading (kN)	Number of cycles	Displ. rate in loading (mm/s)	Displ. rate in unloading (mm/s)
1	120.0	5.0	1	-0.30	0.50
2	150.0	5.0	1	-0.30	0.50
3	175.0	5.0	1	-0.30	0.50
4	200.0	5.0	1	-0.30	0.50

Table 2: load protocol for the TF3 bare frame cyclic test.

4. Experimental results

The monotonic and cyclic tests performed on the TREP elements and TF timber frames were aimed mainly at evaluating their load capacity and ductility. In this regard, the main results are represented by the load-displacement curves obtained from the data recorded by the LVDT located in the horizontal jack "J1".

In addition, expected results from cyclic tests comprised the evaluation of the progressive loss of stiffness and strength at each load cycle until the ultimate conventional displacement was reached. To this aim, the load-displacement curves have been complemented with additional data from the set of LVDT installed on both the rammed earth panel and the timber frame.

4.1 Experimental results for the TF3 timber frame

By following the cyclic loading protocol described in Table 2, a total of 4 loading-unloading cycles were performed on the TF3 timber frame. The load-displacement curve for the cyclic shear load test on the TF3 frame is plotted in Figure 6. To ease the comparison, in the same figure the diagram of the monotonic shear load test on the TF2 frame is also plotted. The horizontal displacements are plotted on the abscissa and the horizontal force is plotted on the ordinate.

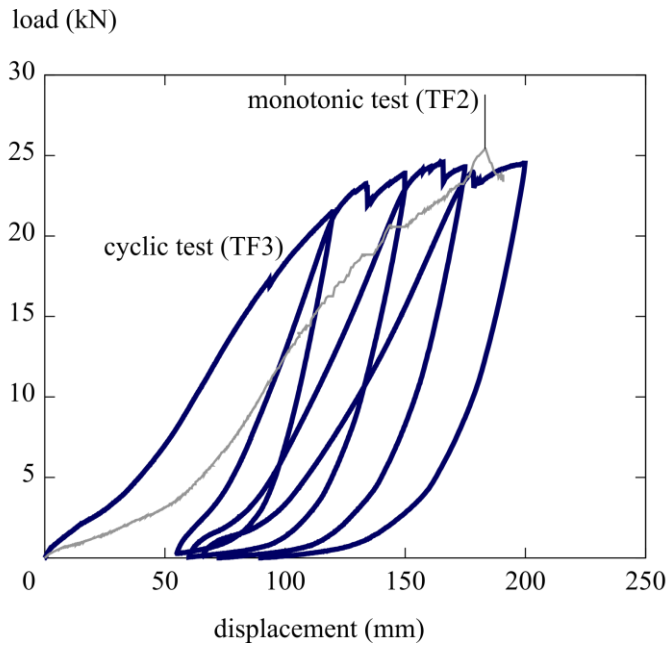

Figure 6: load-displacement curves for the TF2 and TF3 elements.

The diagram can be ideally subdivided into three phases, each corresponding to a different mechanical response of the TF element. Phase 1, going from the origin up to 5 kN, is characterized by an increasing stiffness, mainly due to the reduction of the play between the different parts composing the frame. Phase 2, roughly from 5 kN to 15-17 kN, shows a linear, although inelastic, response of the frame. It is interesting to remark that within this range similar values in the stiffness are observed in all the subsequent loading cycles. Lastly, phase 3 shows a progressive decrease in the stiffness that enables the frames to reach large displacements.

4.2 Experimental results for the TREP3 and TREP4 elements

The load-displacement curves for the cyclic tests are illustrated in Figure 7 in terms of horizontal force and displacement from the "J1" actuator. For the sake of clarity, the diagrams of the monotonic tests are displayed on the background of Figure 7 as shaded gray curves.

The cyclic loading protocol described in Table 1 allowed obtaining a total of 9 cycles were performed for the TREP3 element, while 10 cycles were performed for the TREP4 element. The scheduled tenth cycle was not performed in the case of TREP3 because the ultimate displacement (point D) was reached during the eighth cycle.

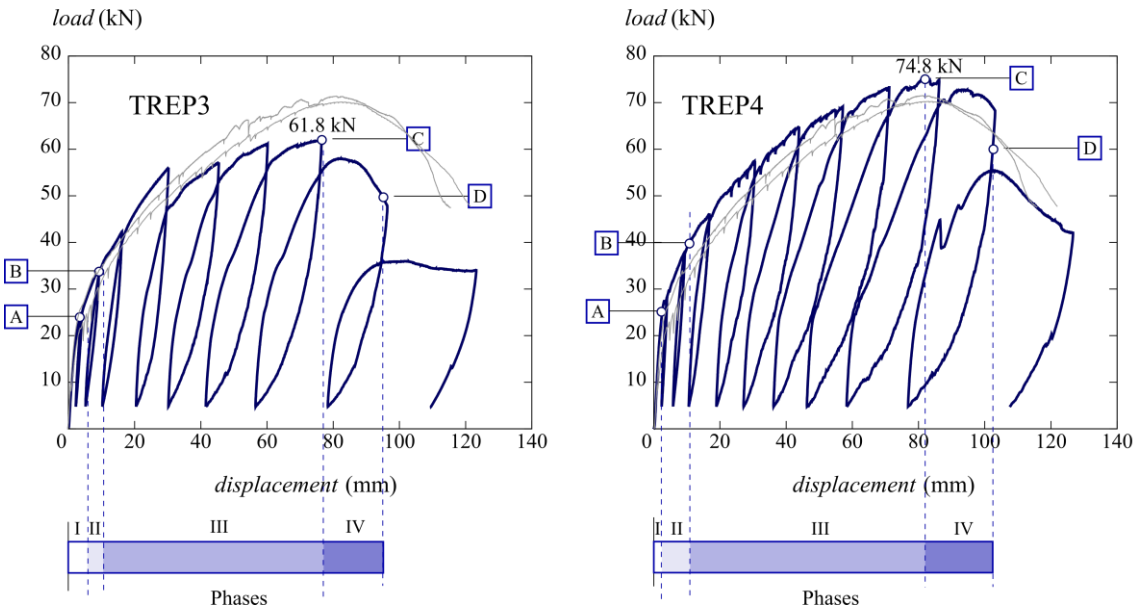

Figure 7: the load-displacement curve for the TREP3 (left) and TREP4 (right) elements.

The large ductility shown by the TREP elements is evident from the diagrams, as well as the progressive strength degradation at each cycle. The horizontal load capacity exhibited in the cyclic tests turned out to be fully compatible with the corresponding values obtained from the monotonic tests, as also illustrated in Fig 7. The TREP4 element turned out to own the higher strength. More specifically, the maximum horizontal load recorded in the TREP4 test is 6 % higher than the mean value obtained in the monotonic tests (70,5 kN), while that of the TREP3 test is 12 % less. The differences observed in the results of the loading tests, although not negligible, can be considered as fully acceptable by considering the many uncertainties in the rammed earth panels building process. In this regard, it's recalled that differences as high as ± 20 % can be observed in analogous experimental researches documented in the literature [11].

Four points indicated with the letters A, B, C, D are highlighted on the diagrams. They ideally subdivide the load-displacement response curve into four phases (phase I-phase IV), each corresponding to a different mechanical response of the TREP element. More specifically, points A, B, C, D are linked to three damage indicators for the TREP elements, namely: (a) the relative vertical displacements between the upper beam and the columns; (b) the relative rotations between the upper beam and the columns; (c) the positive principal strain evaluated at the center of the panel. The load levels corresponding to points A, B, C, D have been determined according to the following:

- Point A corresponds to the first appearance of not negligible values of at least one among the three damage indicators selected for the system.
- Point B corresponds to the appearance of not negligible values of all the three damage indicators selected for the system.
- Point C marks the peak load registered during the test.
- Point D corresponds to the ultimate lateral displacement (lateral load equal to 80 % of the maximum force).

The relative vertical displacement between the upper beam and the frame columns (measured by the F10 and F08 LVDTs, see Figure 4) is related to the damage in the joints due to the high bearing stresses in the wood around the bolts. Also, the relative rotation between the upper beam and the frame columns (measured by the F07, F08, F09 and F10 LVDTs) is related to the damage in the joints due to bearing stresses as well as to local failure of the wood in crushing and shear. Furthermore, the positive principal strain evaluated at the center of the panel (measured by the P01-P06 LVDTs) is related to the onset and development of the diagonal cracking pattern in the rammed earth panel. For a more detailed description of the formulas used for evaluating the three damage indicators, the interested reader is referred to the previous part I on monotonic tests [5].
The coordinates of the relevant points on the load-displacement curves are summarized in Table 3. TREP4 element performed better than TREP3 in terms of both ultimate displacement and load capacity. The differences are very contained, less than some 20 %, and could be probably due to some inaccuracies that affected the vertical load in the initial phases of the test on TREP3 element.

		A	B	C	D
TREP3	Load [kN]	*24.5*	*33.0*	*61.8*	*49.4*
	Displacement [mm]	*4.0*	*9.3*	*76.3*	*95.9*
	Drift [%]	*0.3*	*0.6*	*5.1*	*6.4*
TREP4	Load [kN]	*25.0*	*40.0*	*74.8*	*59.8*
	Displacement [mm]	*4.3*	*10.6*	*86.4*	*102.4*
	Drift [%]	*0.1*	*1.1*	*5.8*	*6.8*
Mean values	Load [kN]	*24.8*	*36.5*	*68.3*	*54.6*
	Displacement [mm]	*4.2*	*10.0*	*81.4*	*99.2*
	Drift [%]	*0.2*	*0.9*	*5.5*	*6.6*

Table 3: summary of the results obtained from the cyclic shear-compression load tests.

The displacement at maximum load for the TREP element, in which the timber frame collaborates with the rammed earth panel in sustaining the loads, turned out to reach 80 mm (Point C in the load-displacement diagram). It is of some interest to recall that a far larger value was obtained for the bare timber frames, which reached their maximum

load for a displacement equal to 200 mm. This finding makes it reasonable to conclude that the good performance observed for the TREP elements are due to the beneficial confining effect that the timber frame exerts on the rammed earth panel rather than to the timber frame additional load capacity.

The diagrams of the three damage indicators for the two cyclic tests are displayed in Figure 8 and Figure 9. As is shown in Figure 8, the first detectable sign of damage concerns the relative rotation between the upper beam and the columns (point A, corresponding to 24.5 kN for TREP3 and 25 kN for TREP4). The last indicator to come out, as the horizontal load increases, is the positive principal strain (Figure 8), which exhibits a sudden increase starting from point B, at 33 kN for TREP3 and 40 kN for TREP4. The relative displacement between the upper beam and the column starts increasing somewhere between points A and B.

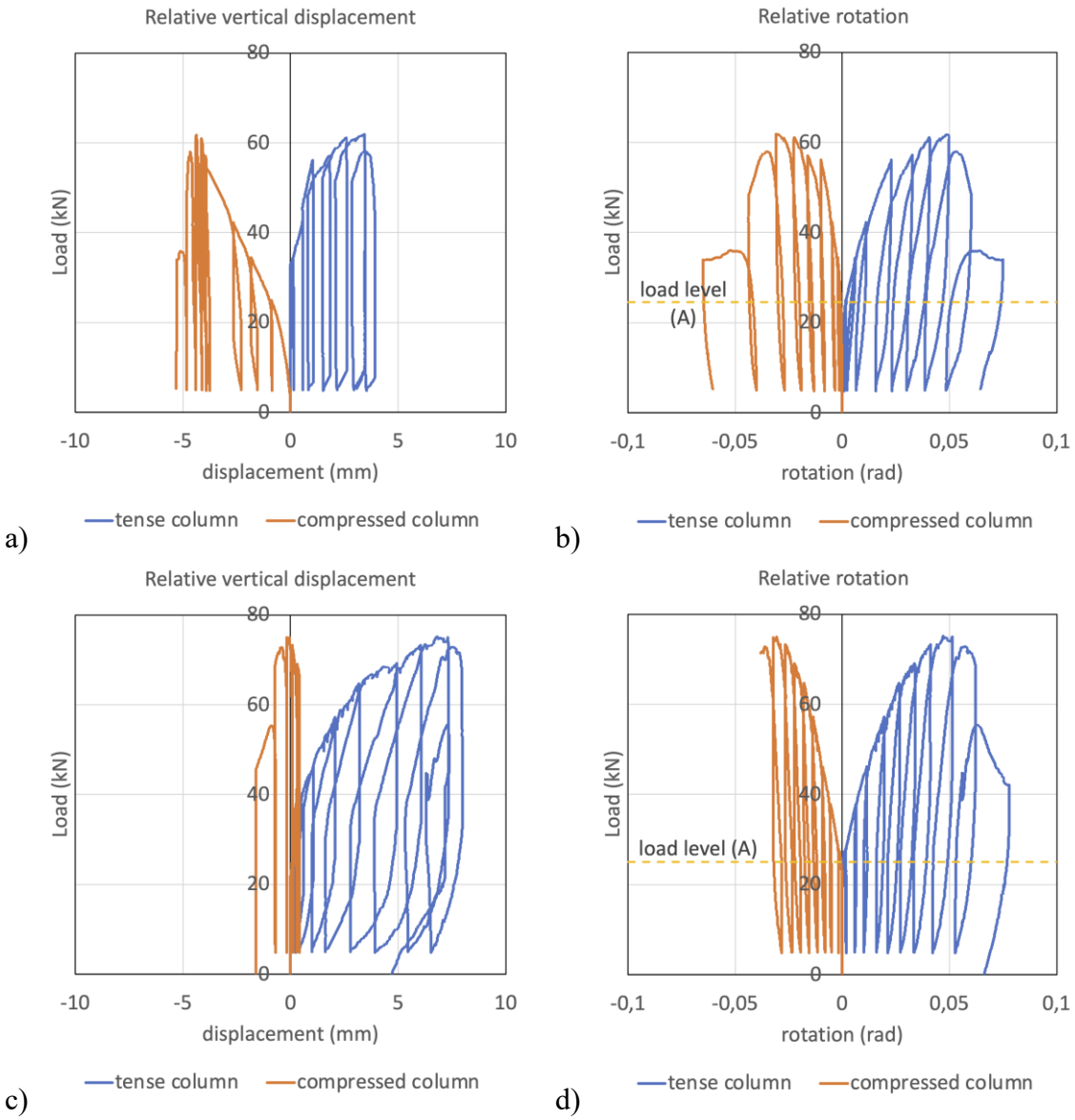

Figure 8: relative rotations and vertical displacements between the upper beam and the frame columns of TREP3 (top diagrams a) and b)) and TREP4 (bottom diagrams c) and d).

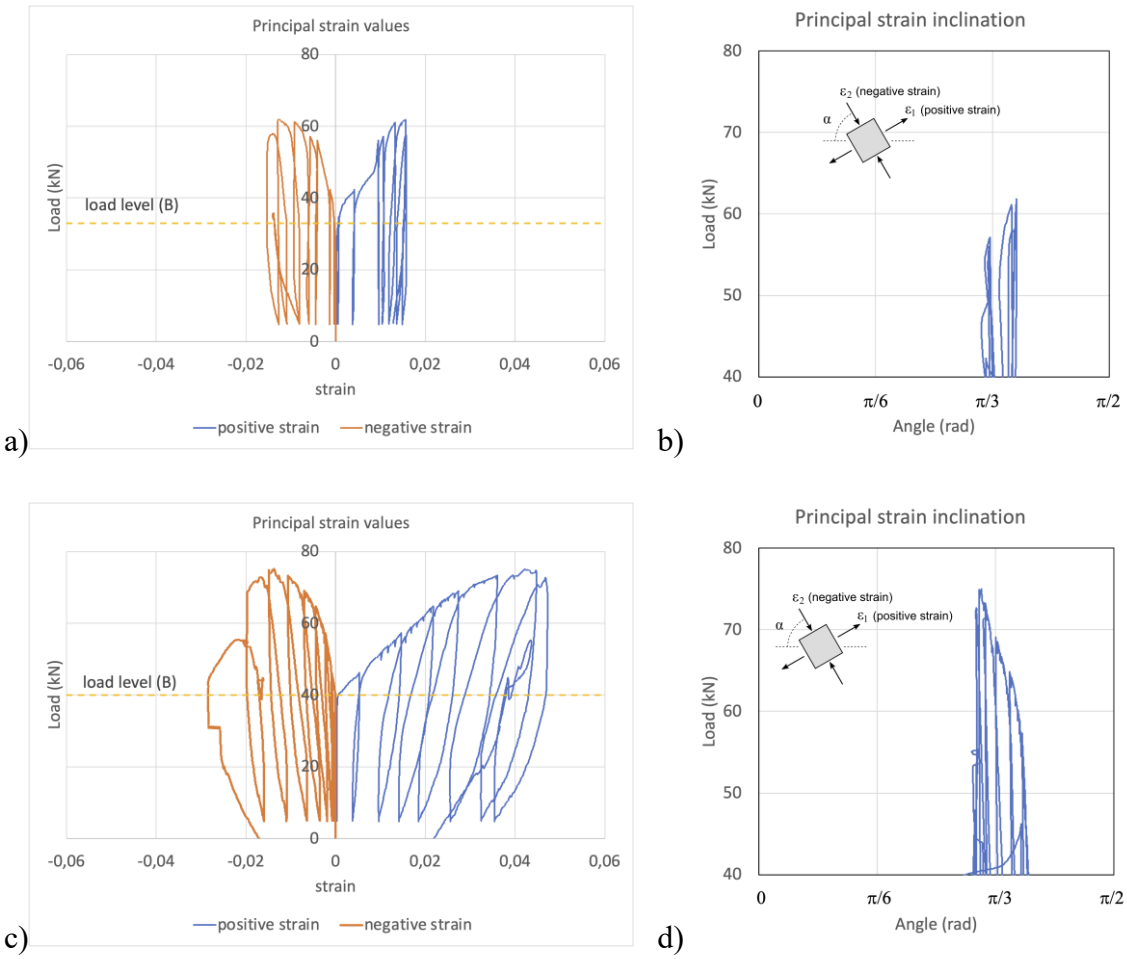

Figure 9: principal strain values (left) and directions (right) in the center of the panel: TREP3 test (figures a) and b)); TREP4 test (figures c) and d)).

By looking at Figure 9, it can be verified that the positive principal strain evaluated at the center of the panel is higher in the TREP4 test. This is likely due to the more pronounced cracking diagonal pattern which developed in TREP4 test with respect to the TREP3 test. This finding is also in agreement with the different horizontal load capacity exhibited by the two panels, as the maximum horizontal load resulted higher for the TREP4 panel.

The results obtained from the tests suggest that the response of the TREP elements is characterized by a first phase (from the origin up to point A) where no relative rotations and displacements between the beam and columns, nor cracks in the center of the panel of appreciable entity appear. These findings agree with the linear trend of the load-displacement curve of the TREP element observed in this load range (Figure 7).

In the second phase (from point A to point B), the damage mechanisms concerning the frame joints (relative rotations and displacements between the beam and columns) activate and start progressing: the upper beam detaches from the columns and contact between the beam and the earth panel is progressively lost. In this phase, the TREP element exhibits a consistent decrease in the tangent stiffness, while the secant stiffness is roughly halved.

In the third phase (from point B to point C), as well as in the fourth and last phase (from point C to point D), further damage accumulates in the joints and a marked diagonal cracking pattern develops on the earth panel. The corresponding load-displacement response of the element is markedly non-linear. In the third phase, the tangent stiffness

of the TREP panel decreases until it becomes approximately zero at point C, which corresponds to the maximum load capacity of the element. In the fourth phase, a softening response is observed, and the negative tangent stiffness continues to decrease until point D is reached, which corresponds to a 20 % decrease in the horizontal load. Point D is considered as the conventional ultimate displacement of the TREP element, beyond which the study of the force-displacement curve is considered as irrelevant.

During the test, the TREP elements suffered progressive damage. The evolution of the damage can be investigated by reporting the trend of some quantities considered structurally relevant. The first quantity to be considered is the total energy (elastic energy plus energy dissipated by the system), corresponding to the area subtended by the force-displacement graph recorded during the test. The total energy (dominated by the dissipated component) is represented as a function of the cumulative displacement, calculated by adding in absolute value all the displacement increments imposed during the test, see Figure 10.

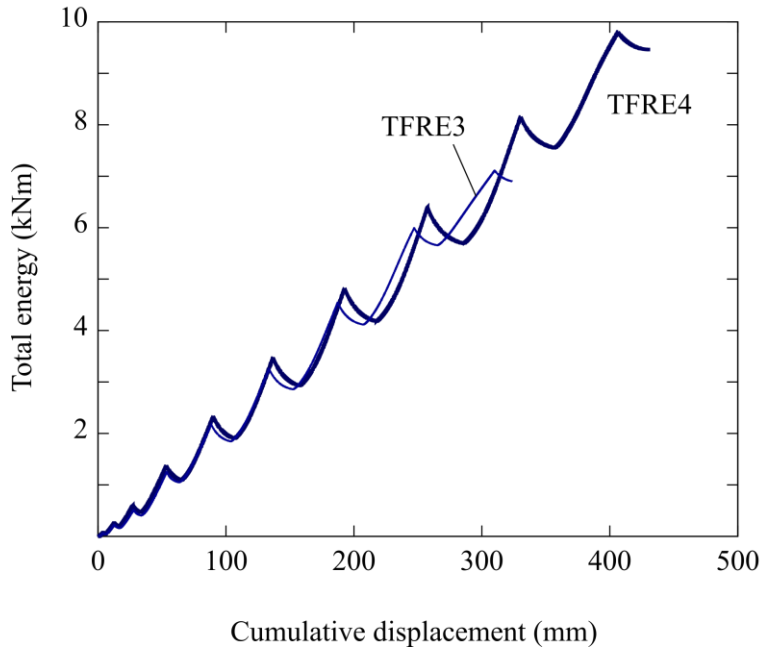

Figure 10: dissipated energy for the TREP3 and TREP4 elements.

Figure 10 clearly shows a progressive increase in the energy, and a direct proportionality between cumulative displacement and energy can be inferred. At the end of the test, an overall cumulative displacement of 323 mm and a dissipated energy of 6.9 kNm have been recorded for the TREP3 element; the corresponding values for the TREP4 elements resulted a bit higher, being equal respectively to 432 mm and 9.46 kNm. The mean energy dissipation ratio can be estimated to be equal to $2.1 \cdot 10^{-2}$ kNm/mm. As already observed, TREP4 element performed better than TREP3, but both specimens exhibited a same curve evolution.

The second quantity to be considered is the strength loss of the TREP elements at each load cycle, graphically represented in Figure 11 for the TREP4 element by the segments A-A', B-B', ..., I-I' on the load-displacement curve. Figure 11 illustrates the strength degradation at each cycle, ΔF, expressed as a percentage of the maximum horizontal force recorded during the test, F_{peak}, as a function of the corresponding displacement, also

expressed as a percentage of the displacement of the element at peak force, d_{peak}. The anomalous value recorded on the TREP3 diagram for d/d_{peak} = 0.4 corresponds to an involuntary temporary change in the vertical load due to an experimental error during the test.

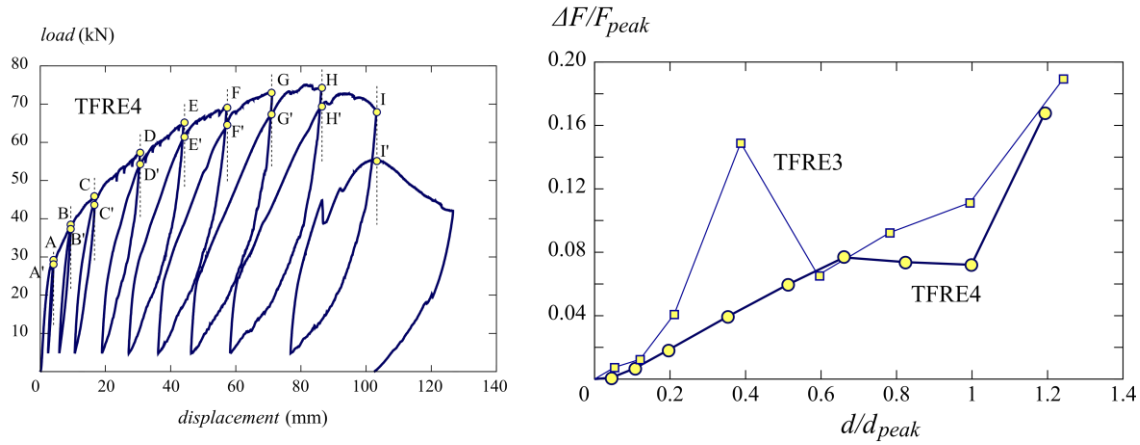

Figure 11: strength degradation at each cycle on the load-displacement curve of the TREP4 element (left); relative values of the strength loss for the TREP3 and TREP4 elements (right).

The last parameter to be considered is the degradation in the stiffness of the TREP elements as the loading cycles grow. The stiffness degradation is evaluated as a percentage of the stiffness at the first cycle. The diagram in Figure 12 shows the stiffness at each loading cycle for the two TREP elements.
By looking at the results of the cyclic loading tests it can be concluded that the TREP elements clearly exhibited a ductile failure, thus confirming the behavior already observed in the monotonic tests. Moreover, a progressive damage in their mechanical properties, without sudden drops in the strength or stiffness has been evidenced.

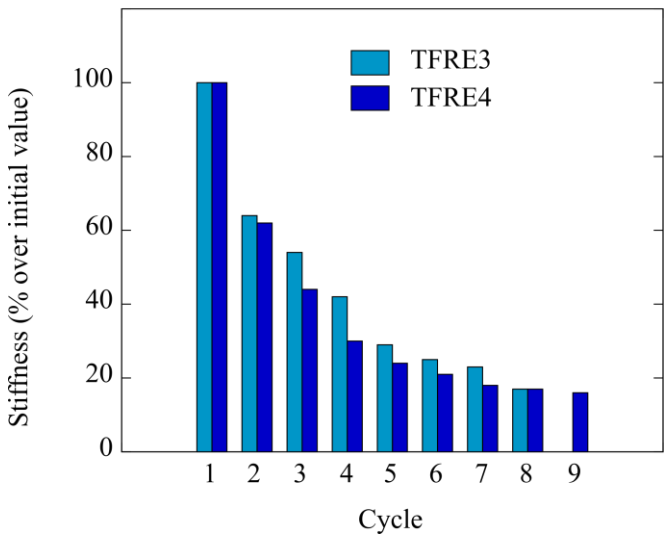

Figure 12: stiffness degradation at each cycle for the TREP3 and TREP4 elements.

4.3 Comparison with relevant literature results

The main results obtained from the tests performed on the TREP elements and on the bare timber frames, TF, are summarized in Table 4 in terms of horizontal load capacity, F_{max}, and the corresponding displacement, δ_{max}, and drift, θ_{max}, for each test. In the last two columns, the ultimate conventional displacement, δ_u, and the corresponding ultimate drift, θ_u, are collected (for the TREP elements only). The mean value and standard deviation of load capacity and ultimate drift of TREP elements are 69.5 ± 5.5 kN and 7.2 ± 0.7 %, respectively.

Test	F_{max} (kN)	δ_{max} (mm)	ϑ_{max} (%)	δ_u (mm)	ϑ_u (%)
TREP1	71.4	80.6	5.4	113.0	7.5
TREP2	70.0	84.5	5.6	121.0	8.1
TREP3	61.8	76.3	5.1	95.9	6.4
TREP4	74.8	86.4	5.8	102.4	6.8
TF2	25.4	183.4	12.2	/	/
TF3	24.5	199.8	13.3	/	/

Table 4: summary of the results of the tests on the TREP elements and the TF timber frames.

The TREP elements exhibited a relevant load capacity. In this regard, a direct comparison with the results documented in the literature does not seem to be possible, as to the authors' knowledge no result is available concerning rammed earth panels confined with timber elements. As a term of comparison for evaluating the TREP elements gain of performance, the results of some experimental tests performed on unreinforced rammed earth panels and documented in the literature [10]-[13] are here considered.

The experimental results collected in Figure 13 clearly show that the maximum horizontal-to-vertical load ratio for unreinforced rammed earth elements can be roughly estimated in the order of 0.5. In the TREP tests, the vertical load imposed on the specimens has been kept equal to 50 kN, and the mean value and standard deviation of the horizontal-to-vertical load ratio turned out to be 1.39 ± 0.11. This finding enables concluding that the performance of the TREP elements is more than doubled when compared to the unconfined elements thanks to the beneficial confining effect of the timber frame.

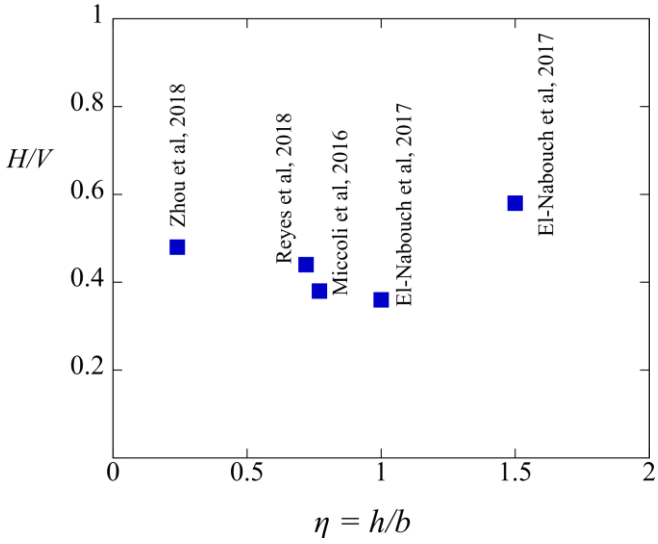

Figure 13: shear-compression tests performed on unreinforced rammed earth panels; horizontal-to-vertical load ratio *vs* panel aspect ratio.

Another point that is worth noting concerns the ultimate drift values of the elements. By referring to the same set of results considered in Figure 13, it can be verified that the ultimate drift values for unreinforced rammed earth panels are less than 2 %. It is of some interest to note that drifts of the order of 1 % have been also determined in mechanical tests performed under different conditions such as in the diagonal compression tests on rammed earth panels documented in [14]. The TREP elements exhibited a far larger ultimate drift capacity equal to 7 %. Hence, the interaction between the earth panel and the timber frame seems to allow for a ductile behavior of the TREP element. It is interesting to observe that very similar drift values have been obtained in the shear loading tests on frames made of wood or bamboo and filled by earth mortar documented in [3].
As already observed in the discussion on the results of the monotonic tests [5], the timber frame exerts a beneficial confinement effect on the earth panel, thus allowing for a diagonal compressive stress field to develop in the panel itself. The very large drift that can be allowed by the timber frame keeps the panel confined until the stresses attain the earth's compressive strength. This enables the TREP element to reach very high horizontal load capacity and drift values compared to the performance of unreinforced elements documented in the literature.
The mechanical response of the TREP elements is strongly affected by the presence of the contouring timber frame. In this regard, it is worth noting that the results of the tests performed on the TREP elements present some similarity with those obtained from the shear test performed on a 1500 mm x 1500 mm x 200 mm rammed earth panel confined by a steel contouring frame hinged at its vertexes, described by Arslan *et al*. [15]. In the cited paper, the maximum load capacity recorded during the shear test, performed without applying any compressive load on the element, turned out to be around 50 kN. If onelooks at the maximum horizontal load per unit thickness, it can be easily checked that both the steel-framed and the timber-framed rammed earth panels got quite similar values, equal respectively to 0.25 kN/mm and 0.28 kN/mm. The small difference between the two values (around 10 %) suggests that the confinement exerted by the frame on the rammed earth panel plays a crucial role in determining the mechanical response of the whole element, and that the level of the vertical compressive load exerted on the panel could be considered a less relevant parameter. However, further experimental tests are needed to address properly this point. In the forthcoming steps of the research, a set of shear-compression loading tests is planned in which the vertical load will be varied.

5. Damage survey in the panel and timber frame

The visual inspection of the TREP elements at the end of the tests enabled recognizing: (a) diagonal cracking in the earth panel; (b) detachment between the earth panel and the contouring timber frame, as well as between the rammed earth layers themselves; (c) crushing and out-of-plane expulsion of the soil; (d) damage in the bolted connections; (e) expulsions of the end part of the upper timber beam due to shear stresses.
The visual inspection of the TF elements at the end of the test allowed to identify damage in the bolted connections and expulsions of the end part of the upper timber beam due to shear stresses.

5.1 Damage survey in the TF elements

The damage survey performed after the loading test on the bare timber frame TF3 enabled recognizing the damage level attained in the joints (Figure 14). As expected, the joints in the bare frames turn out to be more severely damaged with respect to their counterparts

embedded in the TREP elements. Moreover, the damage accumulated during the cyclic test is consistently higher than that in the monotonic test. In this regard, Figure 14 shows large ovalization of the joints due to high bearing stresses in the wood, cracking parallel to the fibers at both the compressed column top and bottom, and expulsion of the end part of the top beam accordingly to a block shear failure mode of the beam-to-column connection.

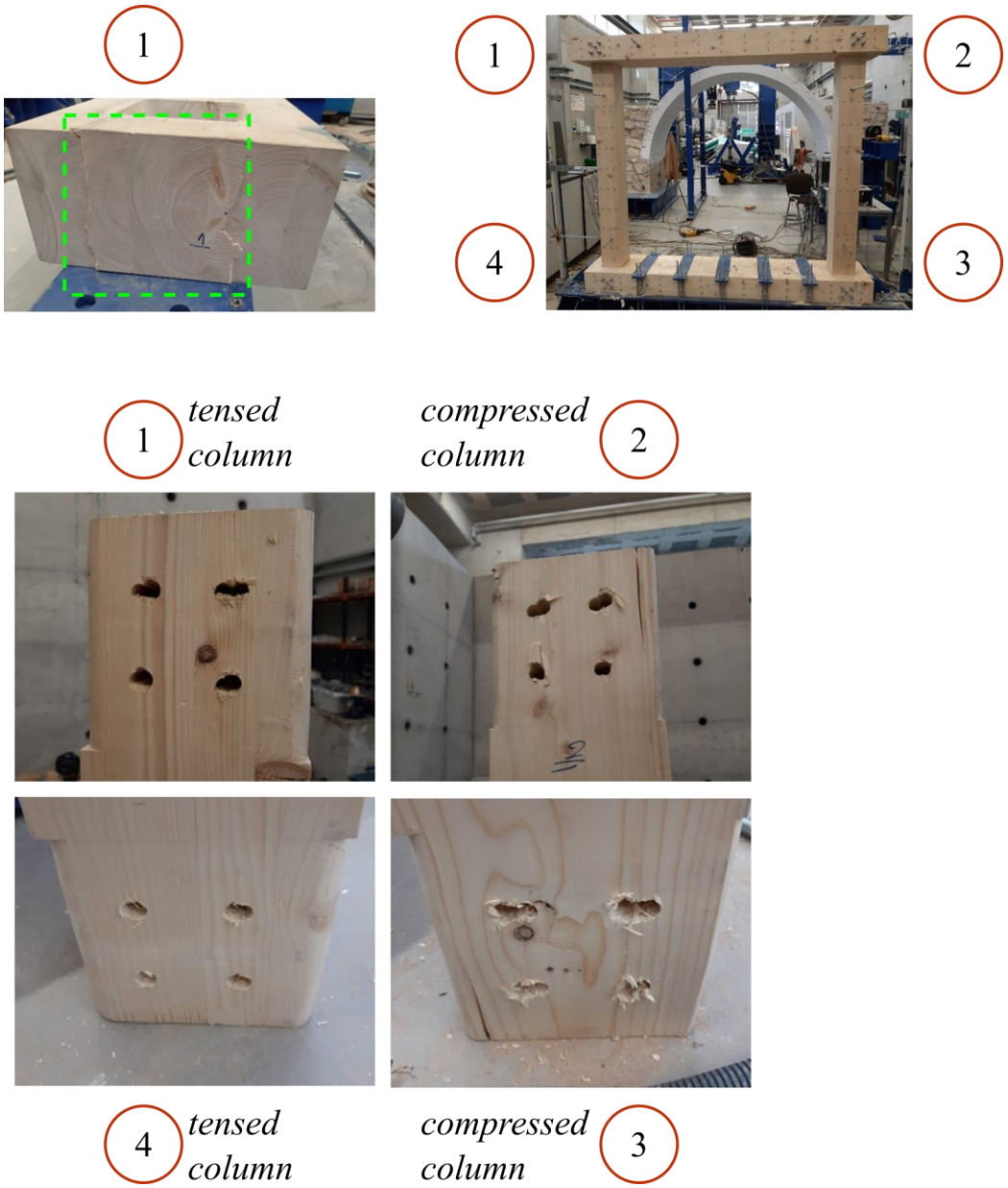

Figure 14: TF3 test – Highlight of the damage in the top beam and joint holes of the timber columns.

5.2 Damage survey in the TREP elements

Figure 15 and Figure 16 show the damage in the rammed earth panel at the end of the TREP3 test. The diagonal cracking is recognizable, as well as the out-of-plane expulsion of a consistent part at the bottom of the earth panel due to compressive stresses. The detachment between the timber frame and the panel is also clearly visible.

Figure 17 shows the conditions at the top and bottom of the timber columns. The columns seem not to be severely damaged, and some light signs of damage can be recognized in the wood around the holes.

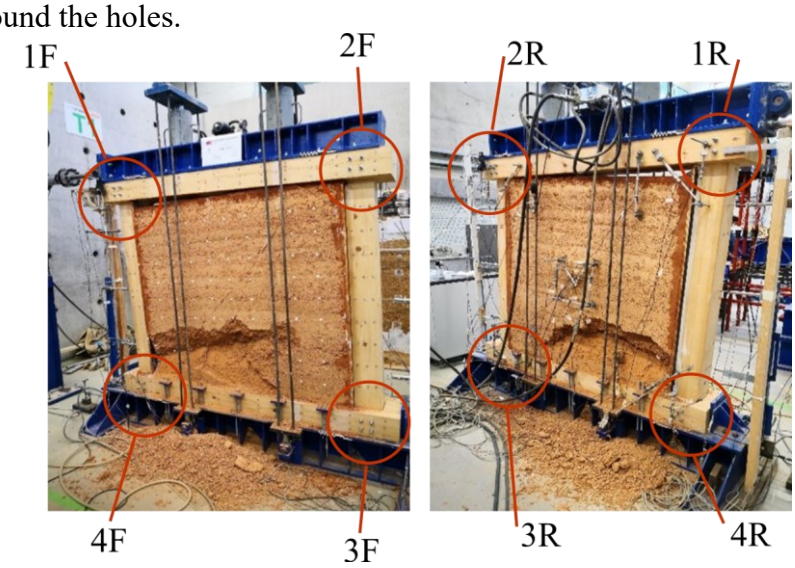

Figure 15: TREP3 test – Highlight of the damage in the rammed earth panel: a) front view; b) rear view.

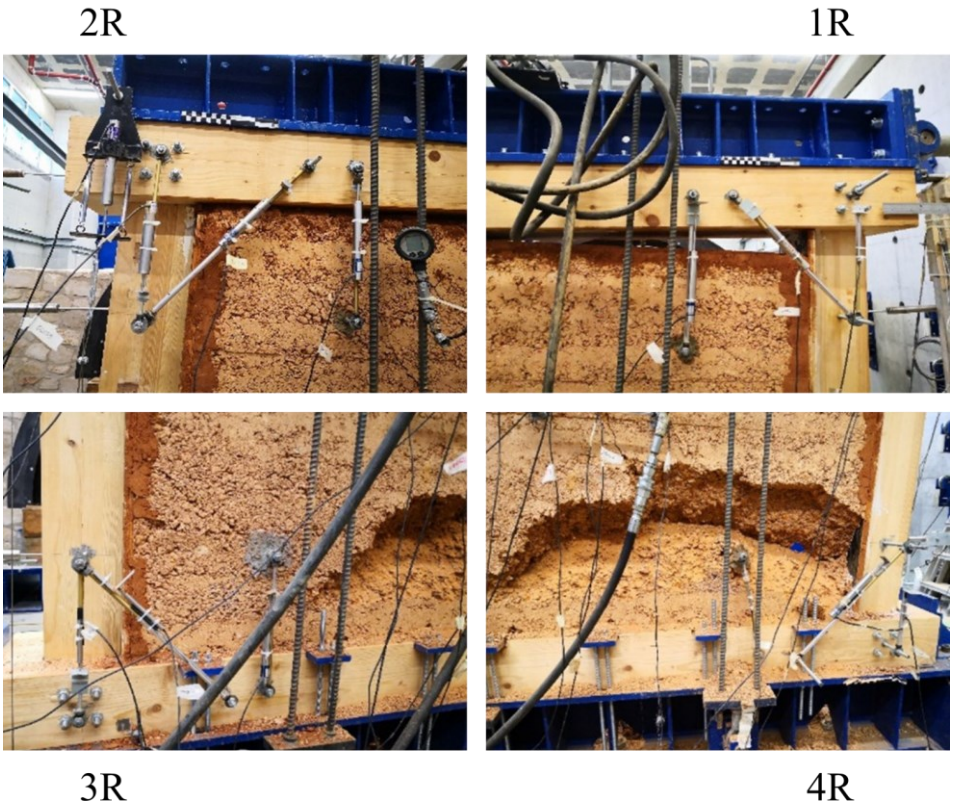

Figure 16: TREP3 test – Highlight of the damage in the corners, rear view.

The damage survey seems to confirm that the collapse of the TREP3 and TREP4 specimens is due to the premature failure of the earth panel, which reached its load bearing capacity while the joints in the timber frame were still able to allow for further load increments. It is worth of some consideration observing that in the TREP4 element, which allowed for higher values of the horizontal load, the local damage in the joints turns out to be more evident, as it will be shown in the following.

Figure 18 and Figure 19 clearly show the damage in the rammed earth panel at the end of the TREP4 test. Once again, the diagonal cracking is recognizable, as well as the out-of-plane expulsion of a consistent part at the bottom of the earth panel due to compressive stresses. The detachment between the timber frame and the panel is also clearly visible. Moreover, some detachment can be seen between the rammed earth layers, in the lower part of the panel.
The experimental damage patterns evidence the development of "strut-and-tie" resisting mechanisms in all samples. In particular, the marked damage observed in the joint holes of the tensed wooden columns (Figure 21) is consistent with this resisting mechanism. The compressed diagonal struts that are formed in the rammed earth panels are easily identified in the cracking pattern shown in Figure 19.

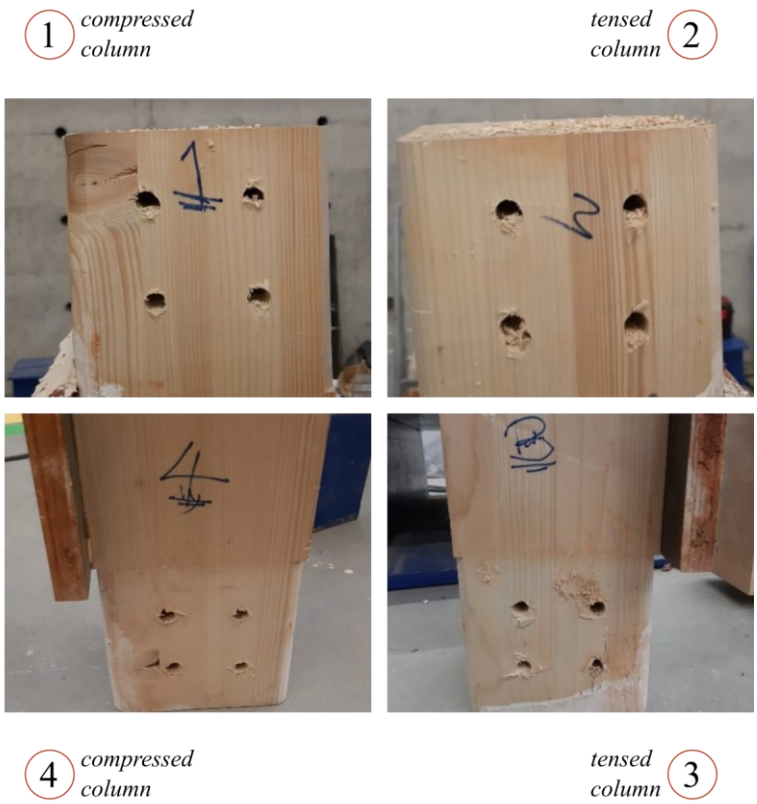

Figure 17: TREP3 test – Highlight of the damage in the joint holes of the timber columns.

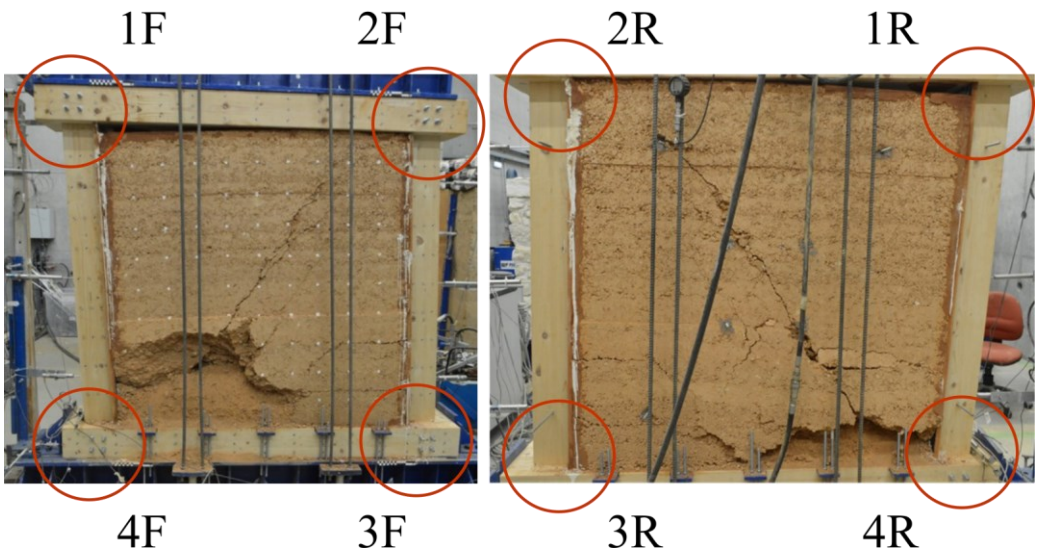

Figure 18: TREP4 test – Highlight of the damage in the rammed earth panel: (a)front view; (b)rear view.

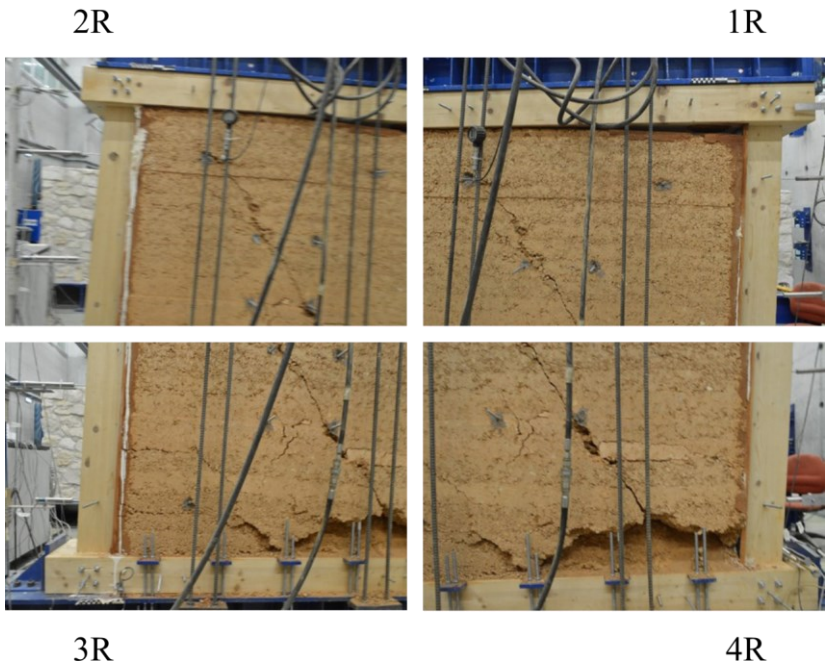

Figure 19: TREP4 test – Highlight of the damage in the earth corners.

Figure 20 enables recognizing that the top beam also suffered some damage at its end in correspondence to the beam-column connection. It seems that the horizontal forces transmitted to the column have reached a limit value corresponding to the onset of a failure mode for the connection, referred as “block shear” in the technical literature [16]. Figure 21 shows the conditions at the top and bottom of the timber columns. In the column under tension some clear signs of damage, which are likely to be due to high bearing stresses, can be recognized in the wood around the holes. In the compressed columns, vertical cracking parallel to the wood fibers, which is likely due to high compressive stresses, can be observed.

The damages detected in the panel and in the frame of the TREP4 element leads to believe that when the horizontal load reached its maximum value a limit condition is attained both in the panel and in the timber frame connections. The comparison between the damage survey of the TREP3 and TREP4 elements seems consistent with the different load capacities observed in the corresponding tests.

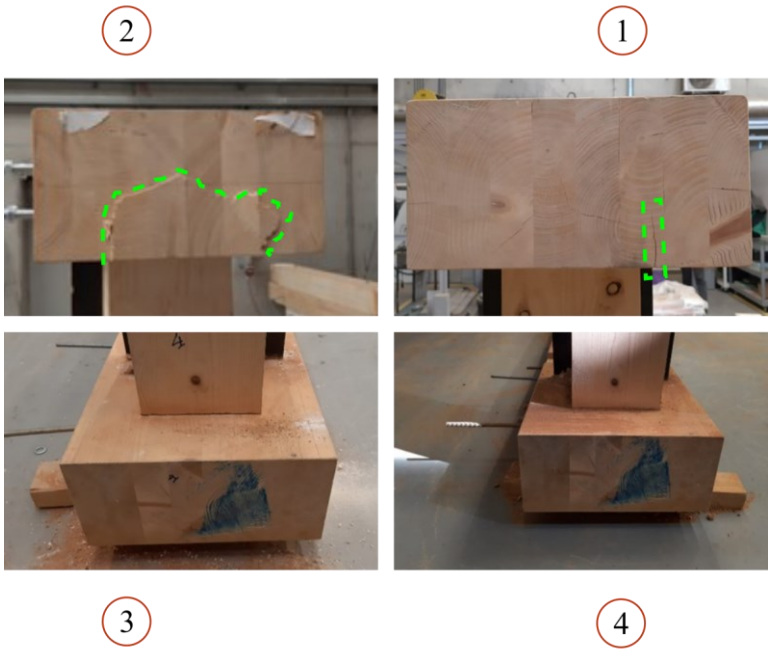

Figure 20: TREP4 test – Highlight of the damage in the timber frame corners.

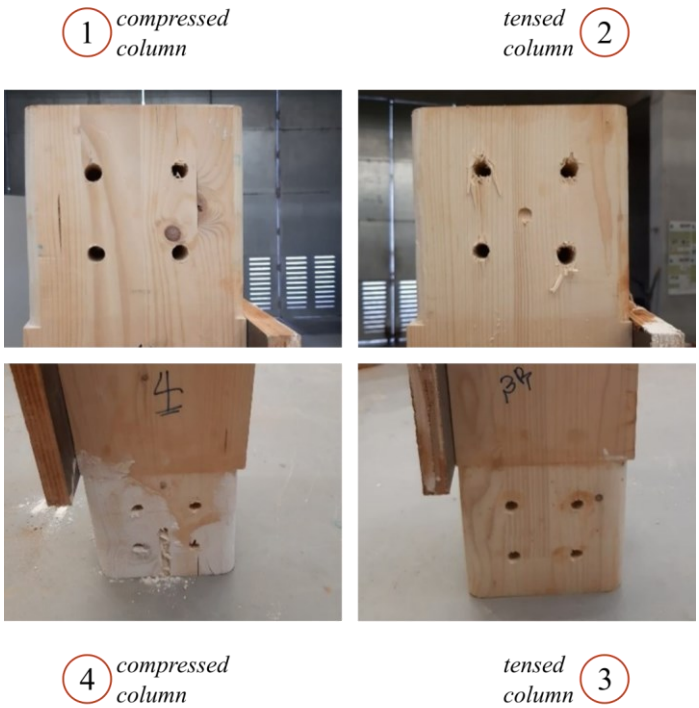

Figure 21: TREP4 test – Highlight of the damage in the joint holes of the wooden columns.

6. Conclusions

In the present two-parts paper, a proposal has been addressed towards the implementation of more sustainable building solutions by exploiting the use of eco-friendly recyclable materials such as "*rammed earth*" in the structural part of the building. Rammed earth walls are usually characterized by comparatively good performances when loaded in compression, as in the case of vertical loads, while their stiffness and strength against horizontal loads are unsatisfactory in many cases. By recovering and readapting traditional strengthening techniques widespread in different countries around the world, this proposal consisted in contouring a rammed earth panel with a reinforcing timber frame, thus making up a composite element indicated as "Timber Framed Rammed Earth" (TREP) endowed with some additional strength and stiffness against horizontal actions.

A first series of experimental loading tests have been set up and performed to the aim of obtaining some preliminary indications about the TREP stiffness and load bearing capacity. The experimental program comprised in-plane monotonic and cyclic shear-compression tests, with the aim of investigating the TREP in-plane static behavior. Loading tests on the bare timber frames have been performed along with those on the TREP elements. The monotonic tests have been illustrated in part I of the paper; the cyclic tests are addressed in the present part II.

The load-displacement curves obtained from the tests on the TREP elements are in very good agreement with each other. The limit values of the horizontal load and drift recorded after the monotonic tests have been substantially confirmed by the cyclic tests. The reinforcing timber frame enabled the development of a "strut-and-tie" resisting mechanism that effectively exploits the compressive strength of the rammed earth panel. Moreover, a progressive loss of stiffness and strength has been observed in the cyclic tests, thus allowing for a ductile failure of the TREP elements. The progressive accumulation of damage in the elements has been also inferred by the amount of the dissipated energy on the system, which increases linearly with the cumulative displacement.

As it was expected, the horizontal load capacity of the TREP elements resulted to be far larger than the corresponding values documented in the literature for unconfined rammed earth panels. It is reasonable to conclude, also based on the results of the tests carried out on the bare timber frames, that the good performance observed for the TREP elements are due to the beneficial confining effect that the timber frame exerts on the rammed earth panel rather than to the timber frame additional load capacity. In this regard, it is worth recalling that the load capacity of the bare frame is attained for a displacement well beyond the ultimate displacement for the TREP element, due to the stiffness of the rammed earth panel.

In conclusion, all the results discussed seem to indicate that the combined use of wood and rammed earth has a significant potential in terms of structural performance, together with a high environmental sustainability. The proposed TREP structural element represents a first prototype on which further studies and research are necessary, especially concerning the detailed design of all its parts. The response of the TREP elements to in-plane vertical and horizontal loading has been certainly encouraging, and the results obtained from the tests even exceeded the best expectations. Nevertheless, the set of loading tests performed so far represents the first step of the research and further study is necessary. The next steps of the research will address the experimental investigation of the out-of-plane response of the TREP elements; further theoretical studies will also be

dedicated to the many mechanical issues involved (timber connections stiffness, damage, and load capacity; timber-panel interactions; rammed earth stiffness and failure criteria) to provide an interpretation of the experimental results and characterize the mechanical behavior of TREP elements.

References

[1] H. Schroeder, (2016). Sustainable Buildings with Earth, Springer International Publishing Switzerland.

[2] M. R. Hall, W. Swaney, (2012). European modern construction, Chapter in: Modern Earth Buildings: Materials, Engineering, Constructions and Applications, Woodhead Publishing Limited, Cambridge, UK.

[3] F. Vieux-Champagne, Y. Sieffert, S. Grange, A. Polastri, A. Ceccotti, A. Daudeville, (2014). Experimental analysis of seismic resistance of timber-framed structures with stones and earth infill, Engineering Structures, 69: 102–115.

[4] H. Cruz, J. S. Machado, A. C. Costa, P. X. Candeias, N. Ruggieri, J. M. Catarino, (2016). Historical Earthquake-Resistant Timber Framing in the Mediterranean Area – Heart 2015, Springer International Publishing Switzerland.

[5] R. Barsotti, S. Bennati, D. V. Oliveira, C. Tirabasso (2021). Experimental investigation of the mechanical response of in-plane loaded Timber-Framed Rammed Earth panels. Part I: monotonic shear-compression tests.

[6] P. Doat, A. Hays, H. Houben, S. Matuk, F. Vitoux, (1979). Construire en terre, CRAterre, Centre de Recherche et d'Application – Terre, Collection AnArchitecture, France.

[7] M. Achenza, U. Sanna, (2006). Il manuale tematico della terra cruda, DEI Tipografia del Genio Civile.

[8] EN 12512:2001. Timber structures - Test methods - Cyclic testing of joints made with mechanical fasteners.

[9] ISO 21581:2010. Timber structures - Static and cyclic lateral load test methods for shear walls.

[10] L. Miccoli, A. Drougkas, U. Muller, (2016). In-plane behavior of rammed earth under cyclic loading: Experimental testing and finite element modelling, Engineering Structures, 125: 144–152.

[11] R. El-Nabouch, Quoc-Bao Bui, O. Plé, P. Perrotin, (2017). Assessing the in-plane seismic performance of rammed earth walls by using horizontal loading tests, Engineering Structures, 145: 153–161.

[12] J. C. Reyes, L. E. Yamin, W. M. Hassan, J. D. Sandoval, C. D. Gonzales, F. A. Galvis, (2018). Shear behavior of adobe and rammed earth walls of heritage structures, Engineering Structures, 174: 526–537.

[13] T. Zhou, B. Liu, X. Zhao, J. Mu, (2018). Experimental testing of the in-plane behavior of bearing modern rammed earth walls, Advances in Structural Engineering: 1–11.

[14] L. Miccoli, D. V. Oliveira, R. A. Silva, U. Muller, L. Schueremans. (2015), "Static behavior of rammed earth: Experimental testing and finite element modelling".

[15] M. A. Arslan, M. Emiroglu, A. Yalama. (2016), “Structural behavior of rammed earth walls under lateral cyclic loading: A comparative experimental study”.
[16] EN 1995-1-1 (2004): Eurocode 5: Design of timber structures - Part 1-1: General - Common rules and rules for buildings.